

Analysis of the Solwind Fragmentation Event Using Theory and Computations

Arjun Tan*

Alabama A&M University, Normal, Alabama 35762

Gautam D. Badhwar†

NASA Johnson Space Center, Houston, Texas 77058

and

Firooz A. Allahdadi‡ and David F. Medina§

Phillips Laboratory, Kirtland Air Force Base, New Mexico 87117

The planned fragmentation of the Solwind satellite in an antisatellite experiment is analyzed from the radar data on the fragments obtained following the experiment. The orthogonal components of the velocity perturbations received by the fragments are calculated, and the angular distributions of the fragments obtained. Groups of three or four fragments having similar velocity changes most likely originated from adjacent parts of Solwind or the antisatellite, and this episode may be an example of sequential fragmentation in space. The angular distribution of the fragments shows a primary and a secondary area of concentration of the fragments, the former possibly indicating the exit area of the antisatellite fragments. Three fragments thrown out with extremely large velocity boosts in the forward direction were objects of much speculation. The possibility that these represented ricochet ejecta resulting from oblique hypervelocity impact between Solwind and the antisatellite is discussed. The velocity of the antisatellite at the moment of impact is estimated to have been near 1 km/s. The angles of encounter, impact, and ricochet are defined and determined. The observed angle between the antisatellite and the ricochet fragments suggests that incidence near 45 deg was possible. The significantly higher ricochet speeds compared with the relative speed between the target and the projectile are consistent with computational results obtained from Lagrangian and Eulerian hydrocodes. The evidence strongly points to the possibility that the three objects were actually ricochet material produced by oblique hypervelocity impact in space.

Nomenclature

A	= constant in great-circle equation
a	= semimajor axis
dv_r, dv_d, dv_x	= orthogonal components of the velocity perturbations of a fragment
e	= eccentricity
h	= height of fragmentation
I	= angle of incidence
i_1	= inclination of Solwind
i_2	= inclination of antisatellite
R	= angle of ricochet
r_0	= radius of the Earth
$v_r, v_d, 0$	= orthogonal components of the velocity of Solwind
v_1	= velocity of Solwind at encounter
v_2	= velocity of antisatellite at encounter
v_{12}	= velocity of Solwind relative to antisatellite
v_{21}	= velocity of antisatellite relative to Solwind
α	= angle of encounter
β	= plane-change angle of anomalous fragments
γ	= launch azimuth
θ	= zenith angle of fragment
λ	= latitude of the fragmentation point
μ	= gravitational parameter
v	= true anomaly
ϕ	= azimuth angle of fragment
ψ	= longitude

Introduction

THE U.S. Air Force solar observation satellite Solwind P78-1 (also referred to as P-78) was launched on Feb. 24, 1979, into a sun-synchronous orbit and was given the international designator 1979-17A.¹ Its primary mission was to carry out solar observation experiments, the main equipment inside being a gamma-ray spectrometer for the Defence Advanced Projects Research Agency.² Six secondary experiments, including three from the U.S. Navy, two from the Air Force, and one from the Army, were also conducted.^{2,3} The six-year mission of Solwind was highlighted by the discovery of six previously undetected sun-grazing comets.⁴ Having greatly outlived its original mission duration of 12 months, the satellite was chosen as a live target for the U.S. antisatellite (ASAT) test program.

On Sept. 13, 1985, an F-15 Eagle jet fighter took off from Edwards Air Force Base, California, attained a height of over 10,500 m, and launched a 5.5-m-long two-stage rocket. The first stage was a Boeing short-range attack missile, and the second stage was a Vought Altair III rocket booster.² After the second-stage burnout, a miniature homing vehicle (MHV) separated from the rocket. Guided by eight infrared sensors and telescopes and powered by 64 small steering jets, the cylindrical-shaped MHV successfully converged on Solwind over the Pacific Ocean. At 20:43 GMT, the two objects collided at a relative speed for about 7 km/s and fragmented into over 300 trackable pieces in perhaps the first and only U.S. ASAT experiment against a live target in space.^{2,5} Telemetry signals from both Solwind (which was still transmitting data) and the ASAT stopped at the same time, confirming the hit. This study analyzes the Solwind fragmentation event from theoretical considerations.

Data

Physical Characteristics of Solwind

The main body of the Solwind satellite was roughly cylindrical and actually composed of two cylinders: an octagonal cylinder fused to a circular one. The overall length of the two cylinders was 1.3 m and the diameter 2.1 m (Ref. 1). Attached to the main body was

Received Nov. 30, 1994; revision received Aug. 3, 1995; accepted for publication Aug. 19, 1995. Copyright © 1995 by the American Institute of Aeronautics and Astronautics, Inc. All rights reserved.

*Professor, Department of Physics.

†Senior Scientist, Space Science Branch.

‡Chief, Space Kinetic Impact and Debris Branch.

§Numerical Analyst, Space Kinetic Impact and Debris Branch.

Table 1 Orbital elements of Solwind and coordinates of the breakup point

Symbol	Physical quantity	Value	Reference
h_a	Height of apogee	548.6 km	7
h_p	Height of perigee	518.1 km	7
a	Semimajor axis	6911.495 km	Calculated
e	Eccentricity	0.0022064	Calculated
Ω	Longitude of ascending node	182°.5017	1
i	Inclination	97°.6346	1
ω	Argument of perigee	99°.4081	1
M	Mean anomaly	260°.9644	1
E	Eccentric anomaly	260°.9622	Calculated
v	True anomaly	260°.8375	Calculated
T	Time period	95.3 min	7
h	Altitude of fragmentation	525 km	7
λ	Latitude of fragmentation	40°N	7
ψ	Longitude of fragmentation	232°E	7

one nearly square solar panel⁶ of area 4.37 m², which translates to a side of 2.1 m. The mass of the satellite proper was¹ 850 kg, and the total mass of the satellite (including the solar panel and peripherals) was⁶ 878 kg. According to the U.S. Air Force University's *Space Handbook*, the surface density of the solar panel was⁶ 4.88 kg/m².

Physical Characteristics of the ASAT

The MHV projectile, which destroyed P-78, was cylindrical in shape, having a length of 33 cm and a diameter of 30.5 cm, and weighed 15.9 kg (Ref. 6). It contained a laser gyroscope for guidance and eight cryogenically cooled infrared detectors for homing. Midcourse corrections were made by 64 single-shot solid-motor rockets.⁶

Orbital Elements of Solwind and Coordinates of the Breakup Point

The orbital elements of Solwind prior to fragmentation and the coordinates of the point of fragmentation have been taken from Refs. 1 and 7 or calculated using standard equations. They are reproduced in Table 1. The state vectors of the ASAT projectile prior to impact are classified information and will remain so indefinitely. Hence not much is certain about the precise direction from which the projectile encountered P-78.

Orbital Elements and Radar Cross Sections of the Fragments

The orbital elements of the fragments as well as their radar cross sections (RCSs) have been taken from the U.S. Air Force Perimeter Acquisition Radar located at Cavalier AFS (PARCS) and the U.S. Space Command (USSPACECOM) radar data. To factor out atmospheric drag effects, the data are propagated backwards to the time of fragmentation by a technique developed by Badhwar and Anz-Meador.⁸

Method of Analysis

Velocity Perturbations of the Fragments

The magnitude and direction of the velocity perturbation of a fragment can furnish valuable information regarding the nature and intensity of a fragmentation. Exact solutions for the orthogonal components of the velocity perturbations have been obtained by Badhwar et al.⁹ To calculate the velocity perturbations imparted to the fragments, it is convenient to use the parent satellite's local frame of reference at the point of breakup. The three orthogonal directions are defined by the radial and downrange directions in the plane of the orbit and the crossrange direction perpendicular to the plane of the orbit and along the angular momentum vector. In this coordinate system, the velocity vector v of the parent satellite has the components v_r , v_d , and 0. Upon fragmentation, the velocity of a fragment, v' , will have the components $v_r + dv_r$, $v_d + dv_d$, and dv_x , where dv_r , dv_d , and dv_x are the velocity perturbation components received by the fragment during the breakup.

Angular Distribution of the Fragments

The angular distribution of the fragments as they emerge from a breakup may be an indicator of the nature of the breakup.¹⁰ This

distribution may be studied by defining two angles akin to the zenith and azimuth angles of spherical coordinates⁹:

$$\theta = \cos^{-1} \frac{dv_r}{dv} \quad (1)$$

and

$$\phi = \tan^{-1} \frac{dv_x}{dv_d} \quad (2)$$

where dv is the magnitude of the velocity perturbation of the fragment.

Velocity of ASAT at Encounter

It is known that the ASAT traversed a suborbital trajectory¹¹ and collided with Solwind near its apogee.¹² Assuming that the velocity of the ASAT was acquired at the surface, one can calculate its velocity v_2 at encounter. From Keplerian geometry of the suborbital ellipse, it can be shown that

$$v_2 = \{(\mu/a)[(1-e)/(1+e)]\}^{1/2} \quad (3)$$

where

$$a = (r_0 + h)/(1 + e) \quad (4)$$

and

$$e = \frac{h}{h + r_0(1 + \cos v)} \quad (5)$$

Here, e is the eccentricity of the suborbital ellipse, and v is the true anomaly at the takeoff point. It δ is the angular distance between the radius vectors of the takeoff point (Edwards Air Force Base) and the breakup point from the center of the Earth, then $v = \pi - \delta$. Further, if (λ_1, ψ_1) and (λ_2, ψ_2) are the coordinates of the subsatellite points, then δ can be calculated from

$$\delta = \cos^{-1}[\sin \lambda_1 \sin \lambda_2 + \cos \lambda_1 \cos \lambda_2 \cos(\psi_2 - \psi_1)] \quad (6)$$

On putting in the values, we obtain $\delta = 9.68$ deg, whence $v_2 = 2.92$ km/s. This would be the velocity of the ASAT at encounter if it traveled on a suborbital elliptical trajectory and its velocity were acquired at the surface. Actually, however, the ASAT deviated from the suborbital ellipse, making a much steeper climb,¹² and its velocity was acquired during the flight. Consequently, the actual value of v_2 is much less than the calculated value, which can therefore be taken as an upper limit on v_2 .

A lower limit on v_2 can be estimated from the velocity of Solwind at encounter v_1 and the velocity of the ASAT relative to Solwind, v_{21} . The path of Solwind was well known, and the velocity of Solwind at encounter is easily calculated to be $v_1 = 7.6$ km/s. Also, it has been widely reported that $v_{21} = 7$ km/s.^{3,11} The lower limit of v_2 is obtained when v_1 and v_2 are parallel, giving $v_2 = v_1 - v_{21} = 0.6$ km/s.

Angle of Encounter

The angle of encounter α defined by the two vectors v_1 and v_2 is an important parameter that can be estimated given v_1 , v_2 , and v_{21} . From the law of cosines as applied to the velocity triangle, one has (cf. Ref. 13)

$$\alpha = \cos^{-1} \left(\frac{v_1^2 + v_2^2 - v_{21}^2}{2v_1 v_2} \right) \quad (7)$$

The angle of encounter, as estimated from Eq. (5), ranges from 50.05 deg for $v_2 = 1.0$ km/s to 66.73 deg for $v_2 = 2.5$ km/s (Table 2).

Table 2 Angle of encounter as a function of ASAT velocity

ASAT velocity v_2 , km/s	Angle of encounter α , deg	Angle between ASAT and ricochet $I + R = 180 - \alpha - \beta$, deg
2.5	66.73	112.72
2.0	65.18	114.25
1.5	61.13	118.32
1.0	50.05	129.40

An alternative method of determining the angle of encounter is from the inclinations of the target and the interceptor orbits, assuming that the ASAT traveled on a great circle. From the spherical breakup triangle, we have⁹

$$\alpha = \cos^{-1} \frac{\cos i_1 \cos i_2 + [(\cos^2 \lambda - \cos^2 i_1)(\cos^2 \lambda - \cos^2 i_2)]^{\frac{1}{2}}}{\cos^2 \lambda} \quad (8)$$

Here i_2 can be calculated from the launch azimuth γ (cf. Ref. 14):

$$i_2 = \cos^{-1}(\sin \gamma \cos \lambda) \quad (9)$$

Since the takeoff point and the breakup point are close, we have approximately

$$\gamma = \tan^{-1} \left(\cos \frac{\lambda_1 + \lambda_2}{2} \frac{\psi_2 - \psi_1}{\lambda_2 - \lambda_1} \right) \quad (10)$$

On substituting the values, one gets $\gamma = -56.83$ deg, $i_2 = 129.88$ deg, and $\alpha = 46.89$ deg. According to Eq. (5), this corresponds to $v_2 = 0.93$ km/s.

The value of i_2 can also be calculated from the ground trace of the interceptor, which is a great circle given (cf. Ref. 15) by

$$\tan \lambda = A \cos(\psi + \varepsilon) \quad (11)$$

The constants A and ε can be determined by substituting from the coordinates of the takeoff and breakup points, giving

$$\varepsilon = \tan^{-1} \left(\cot \frac{\psi_2 - \psi_1}{2} \frac{\tan \lambda_1 - \tan \lambda_2}{\tan \lambda_1 + \tan \lambda_2} \right) - \frac{\psi_1 + \psi_2}{2} \quad (12)$$

and

$$A = \tan \lambda_1 \sec(\psi_1 + \varepsilon) = \tan \lambda_2 \sec(\psi_2 + \varepsilon) \quad (13)$$

whence $i_2 = \lambda_{\max} = \tan^{-1} A$ or $\pi - \tan^{-1} A$ (for retrograde orbits). On substituting the values, we get $i_2 = 132.98$ deg and $\alpha = 47.07$ deg. This corresponds to $v_2 = 0.93$ km/s.

All three analyses suggest that the probable speed of the ASAT was in the neighborhood of 1 km/s and that α was about 50 deg.

Results and Discussion

Gabbard Diagram

Figure 1 (after Refs. 1 and 16) is the Gabbard diagram of 267 objects some 11 h after the breakup. Since the parent satellite's orbit was nearly circular ($e = 0.0022064$), the expected X form is evident in the figure. The collapsing arms for the lower-period orbits indicate orbital decay and rounding of orbits because of atmospheric drag. A close scrutiny of Fig. 1 reveals the existence of groups of three objects (marked 0, 1, and 2) clustered together in more elliptical orbits than the rest. These fragments must have received relatively large velocity perturbations and most likely came from adjacent parts of Solwind or the ASAT. Groups 0 and 1 to the right of the parent's orbit received large posigrade impulses ($dv_d > 0$), whereas group 2 to the left received retrograde impulses ($dv_d < 0$). Groups 1 and 2, situated away from the arms of the cross, were also recipients of large radial-velocity changes (dv_r). However, the most notable are group 0, in highly elliptic and energetic orbits with large orbital periods. They were certainly ejected with the greatest velocity boosts in the forward direction (dv_d). One year later, one was still being tracked, but the other two, having smaller RCSs, were eventually lost.¹⁶ Speculation about the nature of these objects ranged from insulation material¹⁶ to a clamp (private discussion among orbital debris investigators). In this study, we shall examine the possibility

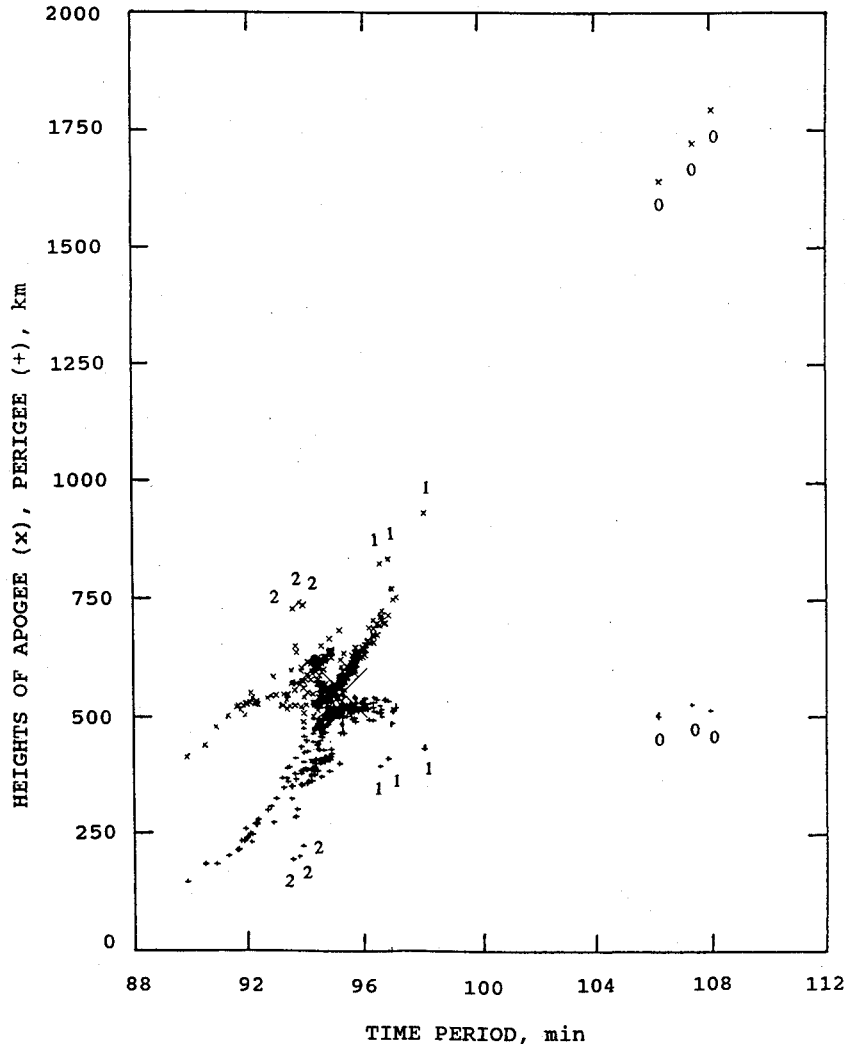


Fig. 1 Gabbard diagram of Solwind fragments.

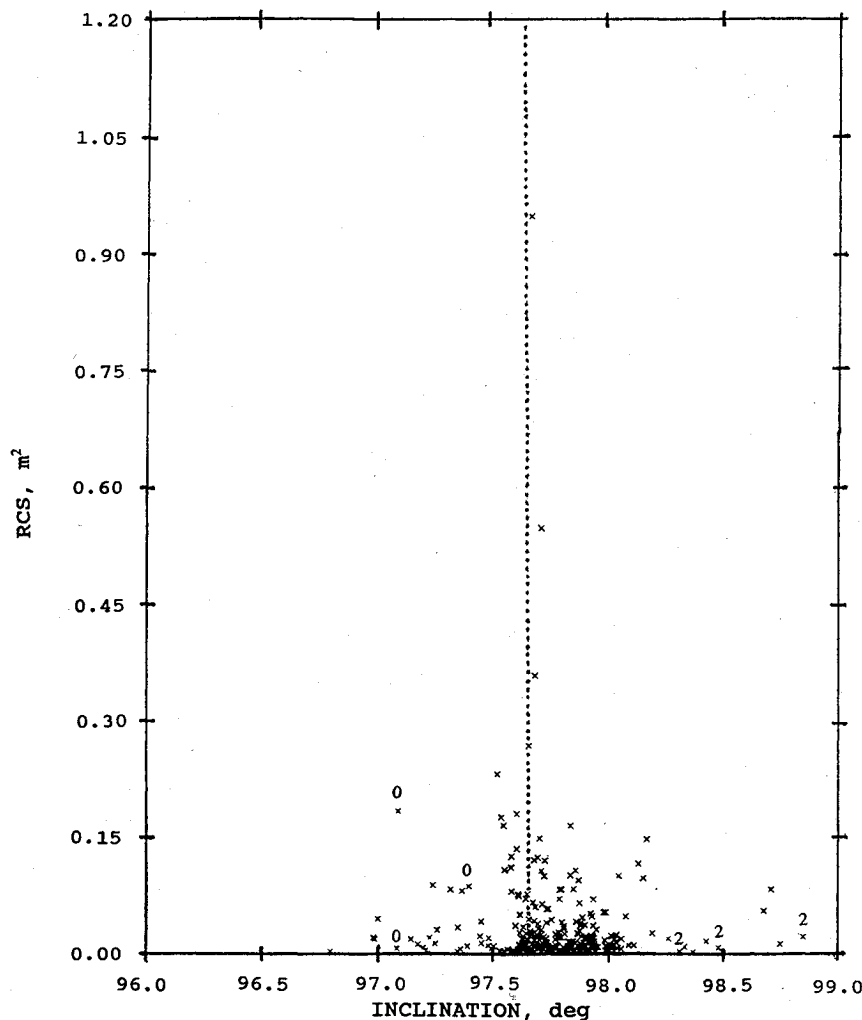


Fig. 2 RCS vs inclination of the Solwind fragments.

that they are ricochet fragments resulting from oblique hypervelocity impact between Solwind and the interceptor.

RCS and Inclinations of the Fragments

Figure 2 (after Ref. 16) is a plot of RCS vs inclination of the Solwind fragments from the PARCS second-pass data. The dotted line marks the inclination of the parent satellite ($i = 97.63$ deg). Two interesting observations can be made from the figure. First, the fragments having the largest RCSs suffered smaller inclination changes than those having smaller RCSs, thus indicating a negative correlation between the inclination change (or, more appropriately, plane change) and RCS. Second, a vast majority of the fragments (including the largest ones) suffered positive inclination changes. Consequently, the net inclination change is positive. This is indicative of a collision with a sizable object. The fragments belonging to groups 0 and 2 are marked in the figure. Their positions indicate that the two groups were ejected on opposite sides of Solwind's orbit.

Velocity Perturbations of the Fragments

Figure 3 (after Ref. 9) is a scatterplot of the three orthogonal components of the velocity changes as calculated from the Cavalier data. This figure, once again, reveals groups of three or four fragments (marked 0, 1, 2, and 3) that had suffered similar velocity changes. As discussed earlier, these objects most probably originated from adjacent parts of Solwind or the ASAT. Figure 3 now provides quantitative meaning to the discussions of the Gabbard diagram. Figure 4 is a three-dimensional plot of the velocity perturbation components. The groups of fragments marked 0 and 2 are identified in the figure. Clearly, group 0 separates itself far apart from the rest of the fragments. For a plausible explanation for a group of fragments to have similar velocity changes, let us recall briefly the basic mechanism

of breakup by hypervelocity impact. The impact generates shock waves in both the target and the projectile, which cause material failure. Cracks are formed by rarefaction waves at the free surface, which propagate rapidly. A volume completely bounded by cracks and/or free surface is detached as a fragment, carrying an initial velocity change with it. In microseconds following the detachment, incomplete cracks in a fragment propagate through it, producing additional fragments, which then acquire further velocity perturbations, but exhibit similar total velocity changes. This episode may well be an example of sequential fragmentation in space. (For a mathematical theory see Ref. 17.)

Angular Distribution of the Fragments

The angular distribution of the fragments is obtained by calculating the angles θ and ϕ for each fragment and plotting them. Figure 5 is analogous to a Mercator projection plot of the fragments. Clearly the distribution is not isotropic. A major concentration area is found around ($\theta_1 = 155$ deg, $\phi_1 = 100$ deg), and a secondary concentration area is found near ($\theta_2 = 100$ deg, $\phi_2 = 80$ deg). To see if they possibly represent the impact and/or exit areas of the ASAT and its fragments, let us analyze the possible areas where the ASAT could have impacted Solwind. At the time of impact, Solwind's axis was along the vertical direction with its solar panel pointing away from the center of the Earth.¹⁸ Even though the ASAT with its infrared sensors was aiming at the solar panel,¹⁸ it is generally believed from the thorough fragmentation of the satellite that the ASAT had actually struck the main body. The angle between the vectors v_1 and v_{12} can be calculated from the velocity triangle (cf. Ref. 13):

$$\xi = \cos^{-1} \frac{v_{21}^2 + v_1^2 - v_2^2}{2v_{21}v_1} \quad (14)$$

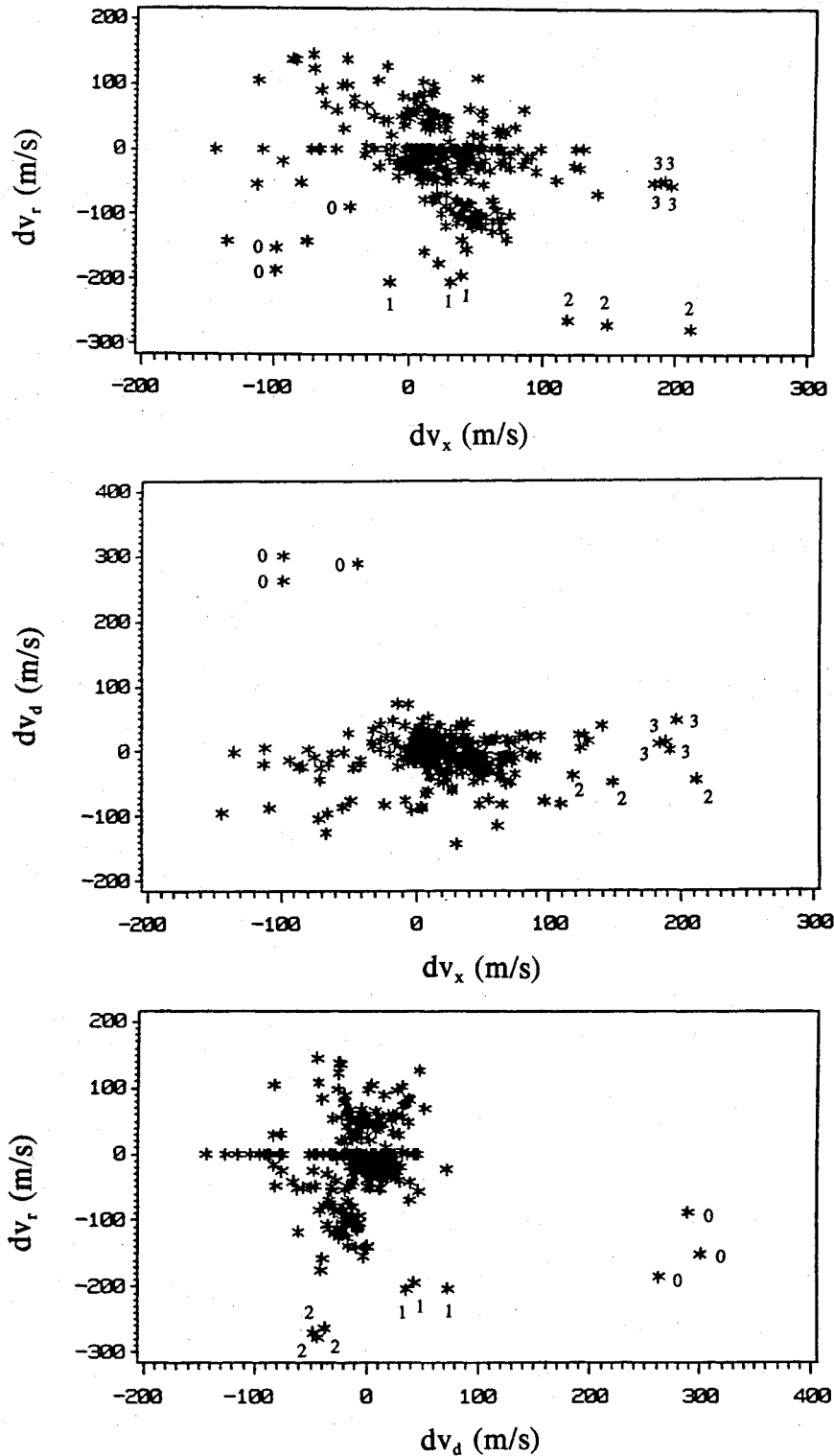


Fig. 3 Scatterplots of the velocity perturbations of the fragments, where dv_r , dv_d , and dv_x are, respectively, the radial, downrange, and crossrange components of the velocity perturbations.

On putting in the values, we find $\xi = 6.29$ deg for $v_2 = 1$ km/s; and $\xi = 5.58$ deg for $v_2 = 0.93$ km/s. Assuming $\xi = 6$ deg, and remembering that Solwind was nearly cylindrical, the possible area of impact of the ASAT is given by -96 deg $< \phi < 84$ deg with maximum impact probability at $\phi = -6$ deg. The primary concentration area ($\phi_1 = 100$ deg) and the secondary concentration area ($\phi_2 = 80$ deg) lie barely outside and inside, respectively, of the probable impact area. While neither of the two areas is likely to be the impact area of the ASAT, the primary concentration area may possibly mark the exit area of the ASAT fragments. There is no proper explanation of the secondary concentration area.

Ricochet Phenomenon in Space?

It is known from Earth-based oblique hypervelocity impact experiments involving fixed targets and small projectiles that secondary ejecta, called ricochet, are produced for incidence angles of 45 deg and greater.^{19,20} It was further reported that the ricochet from 60-deg angle of incidence had greater damage potential than from 45-deg incidence.²¹ The ricochet ejecta are characterized by their high velocities—velocities up to and higher than 30% of the incident projectile velocity have been observed and are predicted by most existing numerical codes, even though published references are hard to locate. Now, the Solwind fragmentation event has been classified as

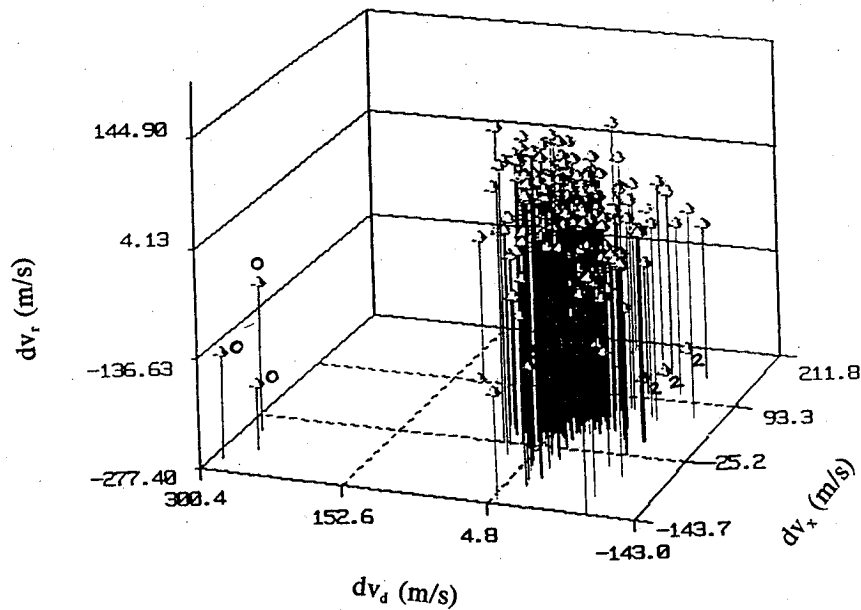


Fig. 4 Three-dimensional plot of the velocity perturbation components, where dv_r , dv_d , and dv_x are, respectively, the radial, downrange, and crossrange components.

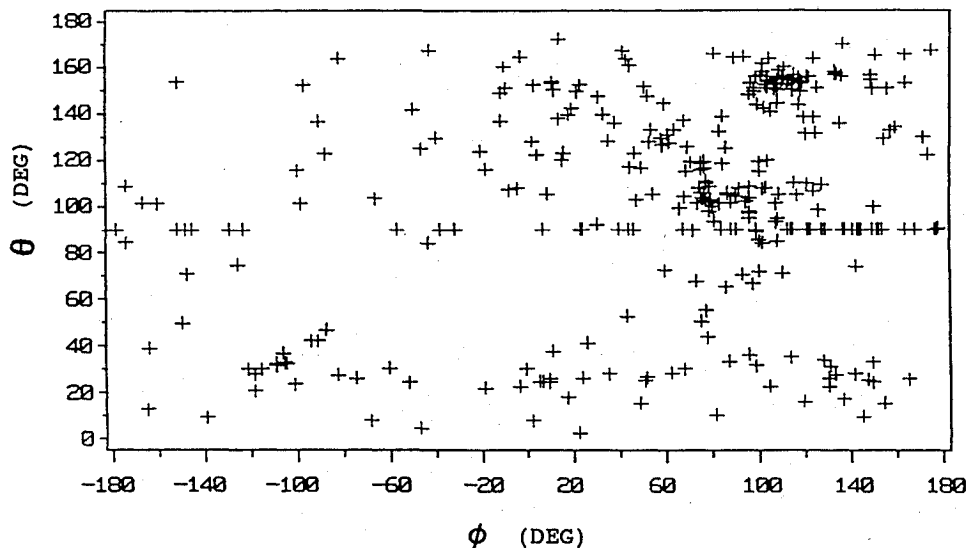


Fig. 5 Angular distribution of the fragments on Mercator projection.

a collision between a large target and a small projectile.¹¹ The group-0 fragments of the Solwind experiment have been called anomalous objects because of their high ejection velocities compared with those of the other fragments. The average velocity of these fragments, 7.89 km/s, is 12.7% higher than the relative velocity between Solwind and the ASAT. That makes these fragments strong candidates for being ricochet fragments in the Solwind breakup event.

To explore this possibility further, let us refer to Fig. 6. For an oblique hypervelocity impact experiment in the laboratory, the angles of impact (I) and ricochet (R) are defined (Fig. 6a) following the customary definitions of the angles of incidence and reflection in geometrical optics. The observed value of R is nearly independent of I and averages about 79 deg (Refs. 19 and 20). Thus, the minimum angle between the incident projectile and the ricochet ejecta is $I + R = 124$ deg, which occurs at $I = 45$ deg (note that the corresponding angle between the incident and ricochet directions is $\pi - I - R$). This angle may now be compared with the angle between the ASAT and the group-0 fragments in the Earth's frame of reference, which is $\pi - \alpha - \beta$ (see Fig. 6b). The average plane-change angle of the group-0 objects is calculated to be $\beta = 0.55$ deg. If the angle of encounter α is uncertain between 50.05 deg (for $v_2 = 1$ km/s) and 66.73 deg ($v_2 = 2.5$ km/s), then $\pi - \alpha - \beta$ is

uncertain between 112.72 and 129.40 deg (Table 2). Since the value $I + R = 124$ deg falls within this range, the group-0 fragments satisfy the minimum-angle criterion established above. Thus, the possibility that the group-0 fragments are actually ricochet material resulting from oblique hypervelocity impact of the ASAT on Solwind at 45–50 deg cannot be ruled out on the grounds of directionality. In fact, the directionality and the enhanced velocities of the group-0 fragments are strong circumstantial evidence that they are ricochet products of the Solwind experiment in space.

The hypervelocity impact phenomenon is currently under study in the U.S. Air Force Phillips Laboratory at Kirtland Air Force Base with two sophisticated numerical hydrocodes: the multidimensional Eulerian code CTH²² and the smoothed particle hydrodynamics Lagrangian code SPH.²³ Results from both codes indicate that the ricochet ejecta attain velocities over 30% higher than the velocity of the incoming projectile. Figure 7 is a polar plot of the calculated ejecta velocities for oblique hypervelocity impact at 45 deg using a two-dimensional SPH code called MAGI. The target was a fixed aluminum plate, and the projectile consisted of a spherical aluminum sphere traveling at a velocity of $v_0 = 6.958$ km/s and incident at an angle of $I = 45$ deg at the plate. The semicircle in Fig. 7 is the locus of points given by $v = v_0$. The ejecta with the highest velocities

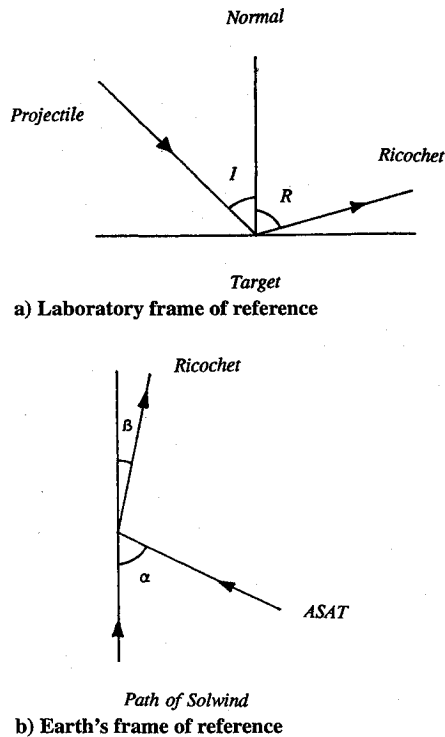


Fig. 6 Geometry of oblique-hypervelocity impact on ground and Solwind fragmentation in space.

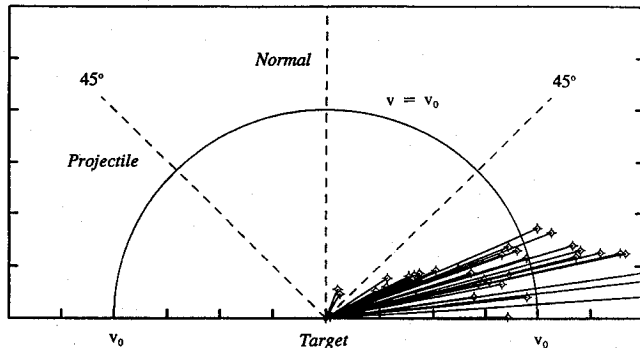


Fig. 7 Ejecta velocity plots for oblique hypervelocity impact of an aluminum sphere traveling at $v_0 = 6.958$ km/s on a fixed aluminum plate at 45-deg angle of incidence according to the Lagrangian MAGI code.

(of up to $1.5v_0$ and higher) are found in the range of R between 65 and 90 deg and around $R = 80$ deg, which agrees fairly well with the experimental values of R . The code further indicates that most of the ricochet material came from the projectile. The computational results now provide additional support to the possibility that the three anomalous objects in the Solwind fragmentation event were ricochet material resulting from oblique hypervelocity impact of the ASAT with Solwind. They also indicate that the fragments most likely originated from the ASAT.

Conclusions

The Solwind fragmentation event is analyzed from the radar data on the fragments obtained following the experiment. The Gabbard diagram and the velocity perturbations plots reveal the existence of groups of fragments having similar velocity changes. The velocity of the ASAT at the moment of impact is estimated by various methods. The possibility that three fragments thrown into high-energy orbits are actually ricochet ejecta resulting from hypervelocity impact between Solwind and the ASAT is discussed. The estimated

angle between the ASAT and the fragments suggests that incidence near 45 deg was possible. The significantly higher velocities of the fragments are consistent with calculated ricochet velocities using both Eulerian and Lagrangian hydrocodes. The evidence strongly supports the possibility that the three objects were actually ricochet material produced by the impact of the ASAT.

Acknowledgments

This study was partially supported by U.S. Air Force Office of Scientific Research Contract F49620-90-C-09076 through subcontract 93-7 from Research and Development Laboratories. The authors wish to thank D. J. Nauer of Teledyne Brown Engineering and N. L. Johnson of Kaman Sciences Corporation for useful discussions, and P. D. Anz-Meador of Lockheed Engineering and Sciences Company, Inc., for assistance in providing data used for this study.

References

- ¹Nauer, D. J., "History of On-Orbit Satellite Fragmentations," 7th ed., Teledyne Brown Engineering, Rept. CS93-LKD-018, July 1993.
- ²Aviation Week and Space Technology, Sept. 1985, pp. 20, 21.
- ³Orbital Debris Monitor, Vol. 2, No. 2, 1989, p. 5.
- ⁴Powell, J. W., "Space Test Programme—an Update," *Journal of the British Interplanetary Society*, Vol. 40, No. 6, 1987, pp. 513–518.
- ⁵Bethel, J., "To Kill or Not to Kill," *Aerospace America*, Nov. 1985, pp. 10–13.
- ⁶Remillard, S. K., "Debris Production in Hypervelocity Impact ASAT Experiments," M.S. Thesis, U.S. Air Force Inst. of Technology, Nov. 1990.
- ⁷Johnson, N. L., and Nauer, D. J., "History of On-Orbit Satellite Fragmentation," 3rd ed., Teledyne Brown Engineering, Rept. CS88-LKD-001, Oct. 1987.
- ⁸Badhwar, G. D., and Anz-Meador, P. D., "Determination of the Area and Mass Distributions of Orbital Debris Fragments," *Earth, Moon, and Planets*, Vol. 45, No. 1, 1989, pp. 29–51.
- ⁹Badhwar, G. D., Tan, A., and Reynolds, R. C., "Velocity Perturbation Distributions in the Breakup of Artificial Satellites," *Journal of Spacecraft and Rockets*, Vol. 27, No. 3, 1990, pp. 299–305.
- ¹⁰Benz, F. J., Bishop, C. V., and Eck, M. B., "Explosive Fragmentation of Orbiting Propellant Tanks," *Proceedings of the Upper Stage Breakup Conference*, NASA Johnson Space Center, Houston, TX, 1987.
- ¹¹Chobotov, V. A., and Spencer, D. B., "Debris Evolution and Lifetime Following an Orbital Breakup," *Journal of Spacecraft and Rockets*, Vol. 28, No. 6, 1991, pp. 670–677.
- ¹²Nauer, D. J., private communication, Teledyne Brown Engineering, 1992.
- ¹³Kessler, D. J., "Determination of Collision Probability Between Orbiting Objects: The Lifetimes of Jupiter's Outer Moons," *Icarus*, Vol. 48, No. 1, 1981, pp. 39–48.
- ¹⁴Bate, R. R., Mueller, D. D., and White, J. E., *Fundamentals of Astrodynamics*, Dover, New York, 1971, pp. 141, 142.
- ¹⁵Fox, C., *An Introduction to the Calculus of Variations*, Dover, New York, 1987, pp. 22–24.
- ¹⁶Kling, R., "Postmortem of a Hypervelocity Impact," Teledyne Brown Engineering, Rept. CS86-LKD-001, Sept. 1986.
- ¹⁷Brown, W. K., "A Theory of Sequential Fragmentation and Its Astronomical Applications," *Journal of Astrophysics and Astronomy*, Vol. 10, No. 1, 1989, pp. 89–112.
- ¹⁸Johnson, N. L., private communication, Kaman Sciences Corp., 1992.
- ¹⁹Schonberg, W. P., and Taylor, R. A., "Penetration and Ricochet Phenomena in Oblique Hypervelocity Impact," *AIAA Journal*, Vol. 27, No. 5, 1989, pp. 639–646.
- ²⁰Schonberg, W. P., "Hypervelocity Impact Penetration Phenomena in Aluminum Space Structures," *Journal of Aerospace Engineering*, Vol. 3, No. 3, 1990, pp. 173–185.
- ²¹Shephard, G. L. Y., and Scheer, S. A., "Secondary Debris Impact Damage and Environment Study," *International Journal of Impact Engineering*, Vol. 14, Nos. 1–4, 1993, pp. 671–682.
- ²²McGlaun, J. M., *CTH User's Manual and Input Instructions*, Version 1.020, Sandia National Lab., 1990.
- ²³Libersky, L. D., and Petchek, A. G., *SPH with Strength of Materials*, CETR, New Mexico Inst. of Mining and Technology, Socorro, NM, 1990.